

### Measurement Uncertainty

The foregoing errors are combined to obtain the precision index, bias limit, and uncertainty for the measurement using equations similar to Eqs. (1-5). As an example, let us analyze a Pratt & Whitney Aircraft RL10 rocket engine force measurement. This force measurement makes up a significant portion of the engine thrust; the remainder is due to pressure and area corrections, because the RL10 is designed to fire in the vacuum of outer space. The test stand force measurement is made with a strain gage load cell system. First we consider the errors resulting from the calibration hierarchy. All errors are expressed as percentages of 12,000 lb, and precision errors are one-standard-deviation ( $1\sigma$ ) values  $b_{11}, \dots, b_{41} = 0.002\%, 0.002\%, 0.011\%, \text{ and } 0.072\%$ ;  $s_{11}, \dots, s_{41} = 0.167\%, 0.034\%, 0.065\%, \text{ and } 0.031\%$ . From Eqs. (5) and (3), respectively,  $B_1 = 0.073\%$  and  $S_1 = 0.186\%$ .

Rather than evaluate each of the errors in the data acquisition and data reduction processes, we have determined the over-all effect of both processes by means of applied load tests. Known forces are applied to the force measurement system with data recorded and reduced to engineering units, utilizing the same procedures employed for acquisition and reduction of run data. In this example, the combined effect of both processes are defined by  $B_2$  and  $S_2$ .

Finally, the over-all uncertainty of the force measurement is computed

$$B_F = 0.12\%, S_F = 0.20\%, U_F = 0.52\%$$

The measured force error must be combined with the nozzle area and pressure correction errors to obtain the RL10 engine thrust uncertainty. This process, called the propagation of error, is described in the following section. The bias and precision index for engine thrust must then be further propagated with propellant measurement errors to obtain the uncertainty for special impulse.

### Propagation of Error

We rarely can measure performance parameters directly; usually we make measurements of more basic quantities like temperature, force, pressure, and fuel flow and calculate the performance parameter as a function of the measurements. The error in the measurements is propagated to the parameter through the function. The effect of the propagation may be approximated with Taylor series methods. These transformations are derived and illustrated in Ref. 1.

### Reference

<sup>1</sup> Interagency Chemical Rocket Propulsion Group Handbook for Estimating the Uncertainty in Measurements Made with Liquid Propellant Rocket Engine Systems, CPIA 180, AD 851127, April 1969.

## A Zoom Maneuver for Descent of Roll Modulated Entry Vehicles

W. FRANK STAYLOR\*

NASA Langley Research Center, Hampton, Va.

**T**HE weight and complexity of terminal descent systems are often a strong function of the dynamic pressure at deployment.<sup>1,2</sup> Drogue parachutes and/or other types of inflatable decelerators are often employed to reduce the dynamic pressure before deployment of the terminal descent system. In the present Note a flight maneuver is described for a roll-

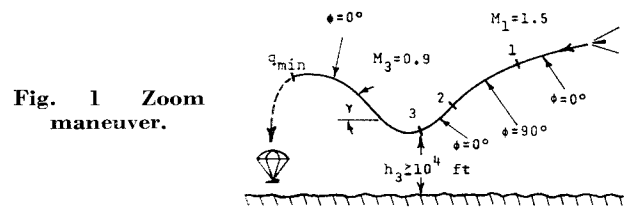


Fig. 1 Zoom maneuver.

modulated, lifting entry vehicle that can drastically reduce the deployment dynamic pressure.

An example of a zoom maneuver is shown in Fig. 1 which is initiated at a flight Mach number,  $M$ , of 1.5 (point 1) by rolling the vehicle from a bank angle,  $\phi$ , of  $0^\circ$  (lift vector up) to  $90^\circ$  (lift vector horizontal). This causes the flight-path angle  $\gamma$  to decrease and the dynamic pressure  $q$  to increase rapidly. At a later flight condition (point 2) the vehicle is rolled back to  $\phi = 0^\circ$ . During this phase of the flight, the vehicle pulls up ( $\gamma$  increases) and  $M$  and  $q$  decrease rapidly.

The third phase of the zoom maneuver is initiated at  $M = 0.9$  (point 3) with a crew-safety restriction that the altitude,  $h$ , be at least 10,000 ft. At this point the vehicle is pitched-up to a high lift attitude, which further increases  $\gamma$  and briefly decreases  $q$  to a minimum value which is considerably less than the minimum value that would be obtained without the pitch-up maneuver. A hypersonic, roll-modulated vehicle could be pitched-up with controls deployed at subsonic speeds ( $M \leq 0.9$ ).

In Fig. 2 the flight conditions at the various maneuver points are given for lift drag ratios  $L/D$  of 1, 2, and 3 ( $M \geq 0.9$ ) for ranges of ballistic coefficient  $W/C_{DA}$ . The flight conditions in Fig. 2a ( $M = 1.5$ ) were determined from equilibrium glide flights ( $\phi = 0^\circ$ ) beginning at  $M = 10$  and are independent of initial re-entry maneuvers. The discontinuities that occur in Figs. 2b and 2c at  $W/C_{DA} \approx 1000$  lb/ft<sup>2</sup> result from the altitude restriction and would occur at higher values of  $W/C_{DA}$  if  $M_1$  were increased.

In Fig. 3 (top) the minimum dynamic pressures  $q_{min}$  are presented for various values of lift coefficient ratio  $C_{L3}/C_{L1}$ , each having a corresponding drag coefficient ratio  $C_{D3}/C_{D1}$  ( $C_L$  and  $C_D$  are  $M \geq 0.9$  values). These ratios are believed

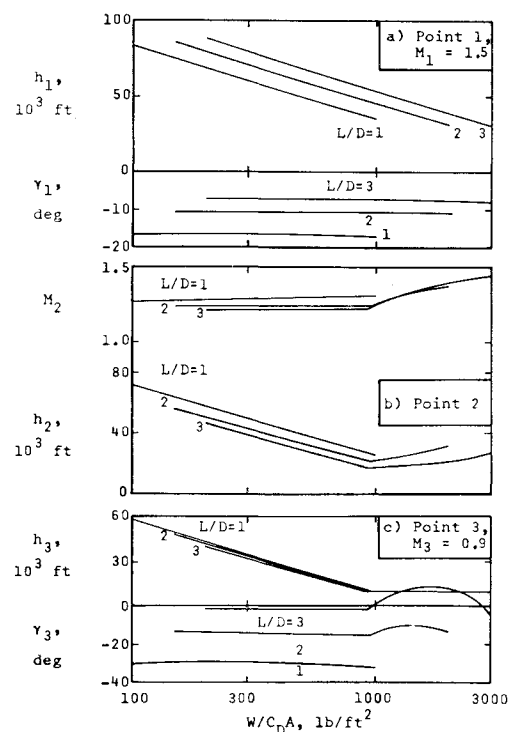


Fig. 2 Flight conditions vs ballistic coefficient for three  $L/D$ 's.

Received August 18, 1969; revision received October 20, 1969.

\* Aero-Space Technologist, Aero-Physics Division. Member AIAA.

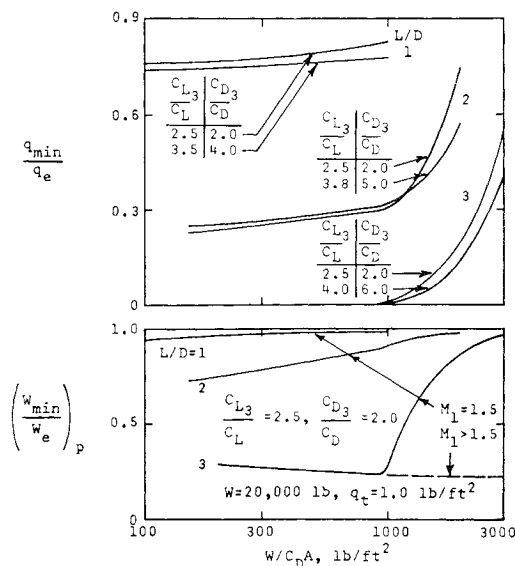


Fig. 3 Minimum dynamic pressures and weights vs ballistic coefficient.

representative of the pitch-up characteristics of lifting entry vehicles at subsonic speeds.  $q_{\min}$  is nondimensionalized by an equilibrium dynamic pressure,  $q_e$ , for  $C_{L3}$  and  $C_{D3}$  conditions ( $q_{\min}/q_e \approx 1$ , if no zoom maneuver is used) defined by the equation

$$q_e = (W/C_D A) [(C_{D3}/C_D)^2 + (L/D)^2 (C_{L3}/C_L)^2]^{-1/2}$$

It is seen that a zoom maneuver reduces  $q_{\min}$  drastically for high-lifting vehicles ( $L/D \geq 2$ ) that are not restricted by altitude limitations ( $W/C_D A < 1000$  lb/ft<sup>2</sup>).  $q_{\min} = 0$  is also obtainable for  $L/D = 3$ ,  $W/C_D A = 3000$  lb/ft<sup>2</sup>,  $C_{L3}/C_L = 2.5$ ,  $C_{D3}/C_D = 2.0$ , for instance, if  $M_1$  is increased to 3.01 ( $q_{\min} = 0$  infers that the vehicle can be pulled-up to  $\gamma = 90^\circ$  and glided to  $M = q = 0$ ).

To illustrate the magnitude of the effect of these reductions in  $q$  on terminal descent systems weights, parachute system weights were determined from the empirical relationships of Ref. 1 for an entry vehicle weight of 20,000 lb and a terminal  $q$  of 1 lb/ft<sup>2</sup>. Figure 3 (bottom) shows  $W_{\min}/W_e$ , the ratio of the weight of a parachute system designed for deployment at  $q_{\min}$  to that of one designed for deployment at  $q_e$ . Little advantage is obtained by use of the zoom maneuver for  $L/D = 1$  class vehicles, but for vehicles with  $L/D = 3$ , a zoom maneuver can reduce the parachute system weight by about a factor near 4, yielding a weight saving of greater than 1000 lb for a 20,000-lb vehicle.

#### References

- <sup>1</sup> Gillis, C. L., "Aerodynamic Deceleration Systems for Space Missions," AIAA Paper 68-1081, Philadelphia, Pa., 1968.
- <sup>2</sup> Staff, "Performance of and Design Criteria for Deployable Aerodynamic Decelerators," TR ASD-TR-61-579, Dec. 1963, Air Force Flight Dynamics Lab.

## Opening Distance of a Parachute

GEORGE C. GREENE\*

NASA Langley Research Center, Hampton, Va.

#### Nomenclature

- $A_i, A_e$  = average effective inlet and exit areas, respectively, during the inflation process  
 $A_{\text{net}}$  =  $A_i - A_e$ , net inlet area

Received May 16, 1969; revision received October 2, 1969.

\* Aerospace Engineer.

- $D_0$  = parachute nominal diameter  
 $L$  = distance traveled during the inflation process  
 $M_\infty$  = parachute Mach number at full inflation  
 $S_p, S_{pf}$  = parachute projected area and value at full inflation  
 $t, t_f$  = time and time interval between snatch force and full inflation, respectively.  
 $V_c$  = volume of parachute canopy  
 $\alpha$  =  $V_c/A_{\text{net}}D_0$ , dimensionless ratio  
 $\gamma$  = ratio of specific heats  
 $\rho_\infty, \rho_T$  = freestream static and stagnation densities, respectively  
 $\rho_{TD}$  = stagnation density downstream of a normal shock  
 $\rho_c$  = density inside canopy at full inflation

#### Introduction

KNOWLEDGE of parachute inflation characteristics is necessary to estimate parachute opening forces. French<sup>1</sup> suggested that the opening distance is a basic parameter in an analysis of parachute inflation characteristics. Based on theoretical considerations of the inflation of a parachute in incompressible flow and subsonic flight test data, he concluded that a given parachute should open in a fixed distance. Reference 2 indicates that the opening distance of a geometrically porous parachute is constant at all Mach numbers for infinite mass deployments; i.e., deployments during which the system velocity remains essentially constant. This Note contains an approximate compressible flow analysis and data from recent NASA programs<sup>3-10</sup> which indicate that although the opening distance may be relatively constant for incompressible flow, it increases with  $M_\infty$  for compressible flow. A technique is presented for predicting opening distances and inflation times for parachutes deployed supersonically based on their subsonic performance.

#### Approximate Analysis and Results

Berndt<sup>11</sup> indicates that a given parachute configuration will exhibit a characteristic canopy area growth with time, i.e., a characteristic curve for  $S_p/S_{pf}$  vs  $t/t_f$  in incompressible flow. By assuming that this characteristic curve is independent of Mach number, one may say that during the inflation process some average value of effective inlet area,  $A_i$ , exists which is constant for a given parachute configuration. It is also assumed that a given parachute will have a constant value of effective exit area  $A_e$ , which will depend on the porosity and porosity distribution in the canopy. Therefore, there will be a net effective inlet area  $A_{\text{net}}$ , which is  $A_i - A_e$ . During the inflation process, a parachute "scoops out" a "column of air" of length  $L$  and average cross-sectional area  $A_i$ . Since part of this column of air  $A_e L$  exits the canopy during the inflation process, the mass of air filling the canopy is  $\rho_\infty L A_{\text{net}}$ . The mass of air in a fully inflated canopy is  $\rho_c V_c$  by definition of  $\rho_c$  and  $V_c$ . Since  $\rho_\infty L A_{\text{net}} = \rho_c V_c$ , the opening distance  $L$  can be expressed as

$$L = (\rho_c/\rho_\infty) V_c / A_{\text{net}} = (\rho_c/\rho_\infty) \alpha D_0 \quad (1)$$

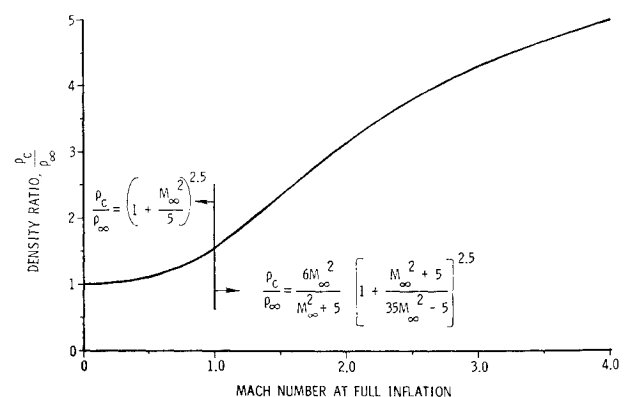


Fig. 1 Variation of density ratio,  $\rho_c/\rho_\infty$ , with Mach number for air ( $\gamma = 1.4$ ).